Electronic Supplementary Information:

Stabilization of optically inactive α-helices of peptidic foldamers through sequence control and *i*, *i* + 4 stapling

Naoki Ousaka,*[a,b], Mark J. MacLachlan*[a,c,d], Shigehisa Akine*[a,e] and Shigenori Fujikawa,*[a,f,g]

[a]Research Center for Negative Emissions Technologies, Kyushu University, 744 Moto-oka, Nishi-ku, Fukuoka 819-0395, Japan. [b]Nano Life Science Institute (WPI-NanoLSI), Kanazawa University, Kakuma-machi, Kanazawa 920-1192, Japan. [c]Department of Chemistry, University of British Columbia, 2036 Main Mall, Vancouver, BC, V6T 1Z1, Canada. [d]Quantum Matter Institute, University of British Columbia, 2355 East Mall, Vancouver, BC, V6T 1Z4, Canada. [e]Graduate School of Natural Science and Technology, Kanazawa University, Kanazawa 920-1192, Japan. [f]International Institute for Carbon-Neutral Energy Research (WPI−I2CNER), Kyushu University, 744 Moto-oka, Nishi-ku, Fukuoka, 819-0395, Japan. [g]Department of Applied Chemistry, Graduate School of Engineering, Kyushu University, 744 Moto-oka, Nishi-ku, Fukuoka, 819-0395, Japan.

E-mail: ousaka.naoki.565@m.kyushu-u.ac.jp (N.O.); mmaclach@chem.ubc.ca (M.J.M.); akine@se.kanazawa-u.ac.jp (S.A.); fujikawa.shigenori.137@m.kyushu-u.ac.jp (S.F.)

Table of Contents

1. Materials and Instruments

Instruments

NMR spectra were measured using a Bruker Ascend 400 spectrometer operating at 400 MHz for ^{1}H and 100 MHz for ^{13}C or a Bruker AVANCE III 600 operating at 600 MHz for ^{1}H and 125 MHz for ^{13}C using tetramethylsilane (TMS) or a residual solvent peak as the internal standard. Electrospray ionization (ESI) time-of-flight (TOF) mass spectra were recorded using a Bruker Daltonics micrOTOF II spectrometer. The high-performance liquid chromatography (HPLC) fractionation and analysis were performed on a Waters 1525 HPLC system equipped with UV-visible detector (Waters 2489) using a COSMOSIL 5C_{18}-MS-II (0.46 (i.d.) × 25 cm for analysis or 2.0 (i.d.) × 25 cm for fractionation, Nacalai Tesque, Kyoto, Japan); MeOH was used as the eluent at a flow rate of 10 mL/min for fractionation and 1.5 mL/min for analysis.

Materials

All starting materials were purchased from commercial suppliers and were used without further purification unless otherwise noted. Silica gel (SiO_2) and aminopropyl-modified silica gel (NH-SiO_2) for the flash chromatography were purchased from Kanto Chemical Co., Inc. and Fuji Silysia Chemical Ltd. (Kasugai, Japan), respectively. Z-(Ac_6c)$_2$-OH,[1] Z-Api(Boc)-(Ac_6c)$_3$-OH,[2] and Z-Api(Boc)-Ac_6c-Aib-OMe[2] were synthesized according to the reported methods.

2. Synthetic Procedures

Abbreviations of chemicals and substituents:

Z: benzyloxycarbonyl,

Boc: *tert*-butoxycarbonyl,

Ac_6c: 1-aminocyclohexanecarboxylic acid,

Api: 4-aminopiperidine-4-carboxylic acid,

HOSu: *N*-hydroxysuccinimide,

COMU: 1-[(1-(cyano-2-ethoxy-2-oxoethylideneaminooxy) dimethylaminomorpholino)] uronium hexafluorophosphate,

EDC·HCl: 1-ethyl-3-(3-dimethylaminopropyl)-carbodiimide hydrochloride,

DIPEA: *N*,*N*-diisopropylethylamine,

General Procedures for the Peptide Syntheses.

Boc- and Z-protecting groups were removed by treatment with 4N HCl in 1,4-dioxane and 10% Pd-C/H_2 in MeOH, respectively. The resulting N- or C-deprotected peptides were used without further purification unless otherwise noted. Peptide coupling reactions were carried out by a COMU method.[3,4]

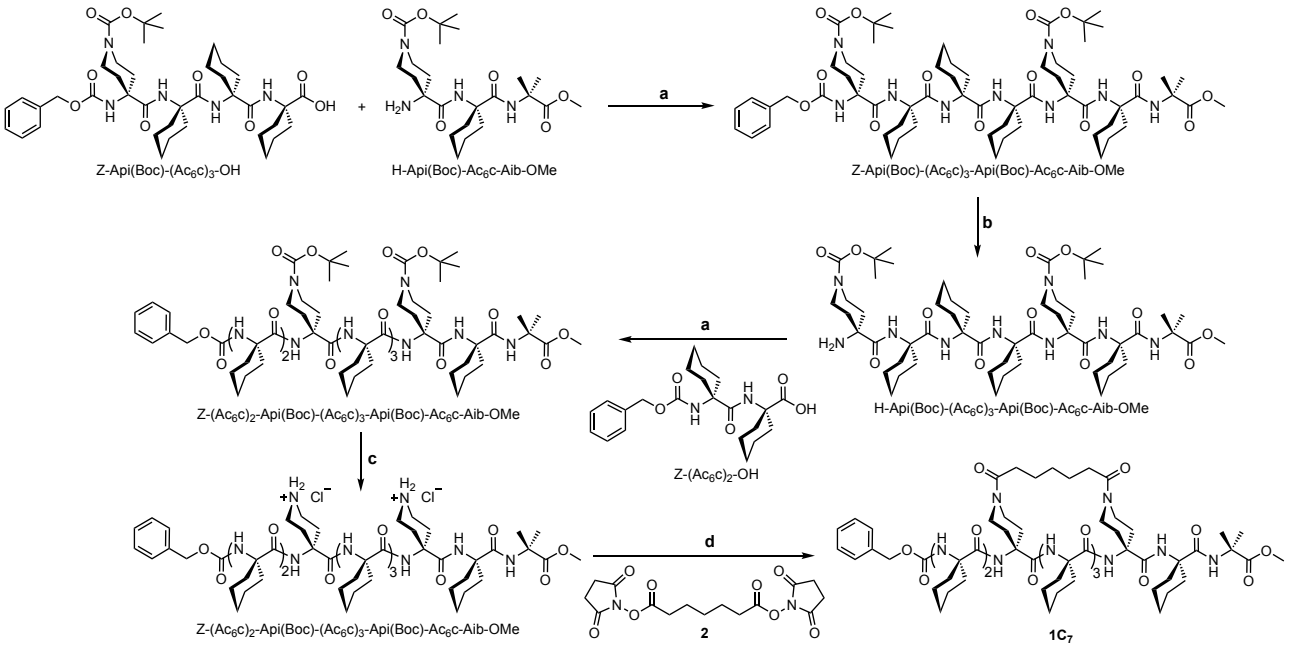

Scheme S1. Synthesis of **1C$_7$**. Reagents and conditions: (a) COMU, DIPEA, CH_2Cl_2, 0 °C to r.t.; (b) 10% Pd-C/H_2, MeOH, r.t.; (c) (*i*) 4N HCl in dioxane, r.t.; (*ii*) DIPEA, DMF, r.t.

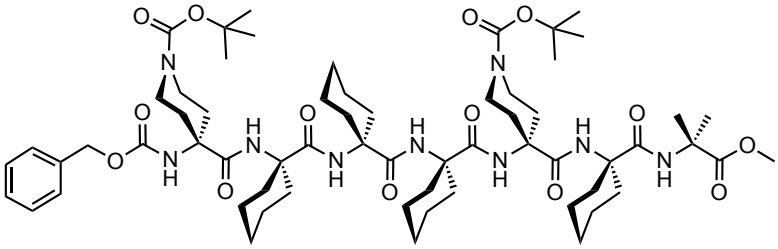

Z-Api(Boc)-(Ac$_6$c)$_3$-Api(Boc)-Ac$_6$c-Aib-OMe: To a suspension of Z-Api(Boc)-(Ac$_6$c)$_3$-OH (1.93 g, 2.56 mmol) and H-Api(Boc)-Ac$_6$c-Aib-OMe (1.20 g, 2.56 mmol), which had been obtained by treatment of Z-Api(Boc)-Ac$_6$c-Aib-OMe with 10% Pd-C/H_2 in MeOH, in dry CH_2Cl_2 (7 mL) was added DIPEA (490 μL, 2.82 mmol) at room temperature. To this was then added COMU (1.10 g, 2.56 mmol) at 0 ºC, and the mixture was stirred at 0 ºC for 2 h and further at room temperature for 16 h under N_2. The solution was diluted with EtOAc, and the mixture was washed with 1N aqueous HCl, 5% aqueous $NaHCO_3$, and brine, dried over $MgSO_4$, filtered, and concentrated under reduced pressure. The residue was purified by recrystallization from EtOAc/*n*-hexane (ca. 1/10, v/v), affording Z-Api(Boc)-(Ac$_6$c)$_3$-Api(Boc)-Ac$_6$c-Aib-OMe as a white solid (2.26 g, 73%). ^{1}H NMR (400 MHz, $CDCl_3$, 25 ºC): δ 7.43 (s, 1H), 7.41–7.32 (m, 6H), 7.12 (s, 1H), 7.02 (s, 1H), 6.98 (s, 1H), 6.55 (s, 1H), 5.49 (s, 1H), 5.16 (s, 2H), 3.90 (bs, 4H), 3.67 (s, 3H), 3.12 (bs, 4H), 2.11–1.25 (m, partially overlapping with H_2O signal). ^{13}C NMR (100 MHz, $CDCl_3$, 25 ºC): δ 176.62, 175.87, 175.57,

175.12, 174.81, 173.83, 173.70, 156.19, 154.75, 154.58, 136.49, 128.71, 128.29, 127.08, 79.98, 79.37, 66.80, 60.15, 59.57, 59.31, 58.98, 58.37, 58.29, 55.84, 52.01, 39.83 (br), 39.40 (br), 28.51, 28.47, 25.67, 25.47, 25.28, 25.01, 21.57 (br). HRMS (ESI-TOF+): *m/z* calcd for ($M+Na^+$), 1226.7047; found, 1226.7131.

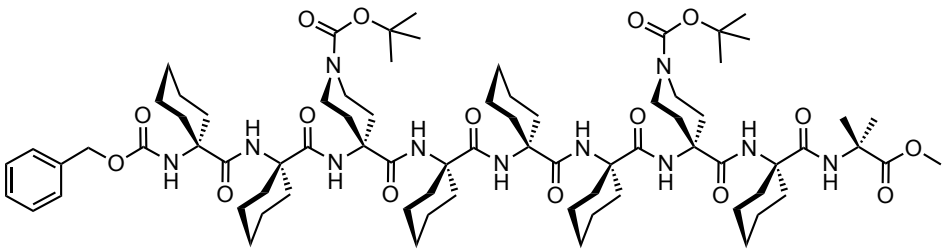

Z-(Ac_6c)$_2$-Api(Boc)-(Ac_6c)$_3$-Api(Boc)-Ac_6c-Aib-OMe: To a solution of Z-(Ac_6c)$_2$-OH (761 mg, 1.89 mmol), H-Api(Boc)-(Ac_6c)$_3$-Api(Boc)-Ac_6c-Aib-OMe (1.76 g, 1.64 mmol), which had been obtained by treatment of Z-Api(Boc)-(Ac_6c)$_3$-Api(Boc)-Ac_6c-Aib-OMe with 10% Pd-C/H_2 in MeOH, and DIPEA (362 μL, 2.08 mmol) in dry CH_2Cl_2 (6 mL) was added COMU (810 mg, 1.89 mmol) at 0 ºC. The mixture was stirred at 0 ºC for 2 h and further at room temperature for 16 h under N_2. The solution was diluted with EtOAc, and the mixture was washed with 1N aqueous HCl, 5% aqueous $NaHCO_3$, and brine, dried over $MgSO_4$, filtered, and concentrated under reduced pressure. The residue was purified by column chromatography (SiO_2, EtOAc/CH_2Cl_2 (1/1, v/v)), affording Z-(Ac_6c)$_2$-Api(Boc)-(Ac_6c)$_3$-Api(Boc)-Ac_6c-Aib-OMe as a white solid (1.70 g, 62%). ^{1}H NMR (400 MHz, $CDCl_3$, 25 ºC): δ 7.48 (s, 1H), 7.38–7.30 (m+s, 6H), 7.23 (s+bs, 2H), 7.17 (s, 1H), 7.10 (s, 1H), 7.00 (s, 1H), 6.48 (s, 1H), 5.56 (s, 1H), 5.16 (s, bs), 3.92–3.89 (m, 4H), 3.67 (s, 3H), 3.06–1.24 (m, partially overlapping with H_2O signal). ^{13}C NMR (100 MHz, $CDCl_3$, 25 ºC): δ 176.69, 176.04, 175.97, 175.82, 175.03, 174.97, 174.64, 174.45, 173.69, 156.14, 154.73, 154.50, 136.74, 128.79, 128.20, 126.53, 79.75, 79.17, 66.84, 60.14, 59.95, 59.56, 59.34, 58.74, 58.33, 57.47, 55.81, 51.96, 39.83, 39.13, 35.10, 28.51, 28.48, 25.69, 25.52, 25.48, 25.38, 25.02, 24.94, 21.72, 21.35. HRMS (ESI-TOF+): *m/z* calcd for ($M+Na^+$), 1476.8728; found, 1476.8800.

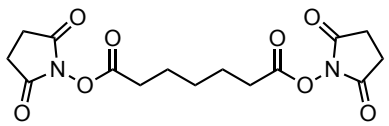

2: To a solution of pimelic acid (1.00 g, 6.24 mmol) and *N*-hydroxysuccimide (1.51 g, 13.11 mmol) in dry CH_2Cl_2 (50 mL) was added EDC·HCl (2.39 g, 12.5 mmol) at 0 ºC. The reaction mixture was stirred at 0 ºC for 1 h and further at room temperature for 18 h under N_2. The solvent was evaporated to dryness under reduced pressure and the residue was dissolved in EtOAc. The solution was washed

with 1N aqueous HCl, 5% aqueous $NaHCO_3$, and brine, dried over $MgSO_4$, filtered, and concentrated under reduced pressure. Purification by recrystallization from EtOAc/*n*-hexane (ca. 1/3, v/v) afforded title compound **2** (1.69 g, 76%) as a white solid. ^{1}H NMR (400 MHz, $CDCl_3$, 25 ºC): δ 2.83 (s, 8H), 2.64 (t, J = 7.4 Hz, 4H), 1.80 (quin, J = 7.8, 7.5 Hz, 4H), 1.58-1.52 (m, partially overlapping with H_2O signal). ^{13}C NMR (100 MHz, $CDCl_3$, 25 ºC): δ 169.28, 168.48, 30.72, 27.86, 25.66, 24.13. HRMS (ESI-TOF+): *m/z* calcd for ($M+Na^+$), 377.0955; found, 377.0959.

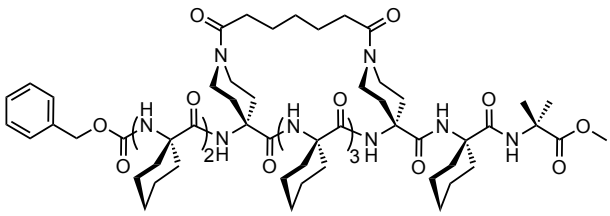

1C$_7$: To a solution of Z-(Ac_6c)$_2$-Api(HCl)-(Ac_6c)$_3$-Api(HCl)-Ac_6c-Aib-OMe (200 mg, 0.151 mmol), which had been obtained by treatment of Z-(Ac_6c)$_2$-Api(Boc)-(Ac_6c)$_3$-Api(Boc)-Ac_6c-Aib-OMe with 4N HCl in 1,4-dioxane, and **2** (58.7 mg, 0.166 mmol) in dry DMF (30 mL) was added DIPEA (79 μL, 0.452 mmol) at room temperature. The reaction mixture was stirred at room temperature for 19 h under N_2. The solvent was evaporated to dryness under reduced pressure and the residue was dissolved in CH_2Cl_2. The solution was washed with water, 1N aqueous HCl, and brine, dried over $MgSO_4$, filtered, and concentrated under reduced pressure. Purification by column chromatography (NH_2-SiO_2, CH_2Cl_2/MeOH (9/1, v/v) and further by reverse-phase HPLC using a COSMOSIL 5C18-MS-II (2.0 (i.d.) × 25 cm, Nacalai Tesque, Kyoto, Japan), afforded title compound **1C$_7$** (120 mg, 60%) as a white solid. The ^{1}H NMR spectral pattern of **1C$_7$** in 1,1,2,2-tetrachloroethane-d_2 (TCE-d_2) at 298 K was complicated, due to the presence of many possible orientations of side-chain amide carbonyl –CO-N(CH_2)– groups that slowly interconvert on the NMR time scale (Figure S9). HRMS (ESI-TOF+): *m/z* calcd for ($M+Na^+$), 1400.8204; found, 1400.8261.

Supporting Data

3. ESI-TOF Mass Spectrum and HPLC Chromatogram of $1C_7$

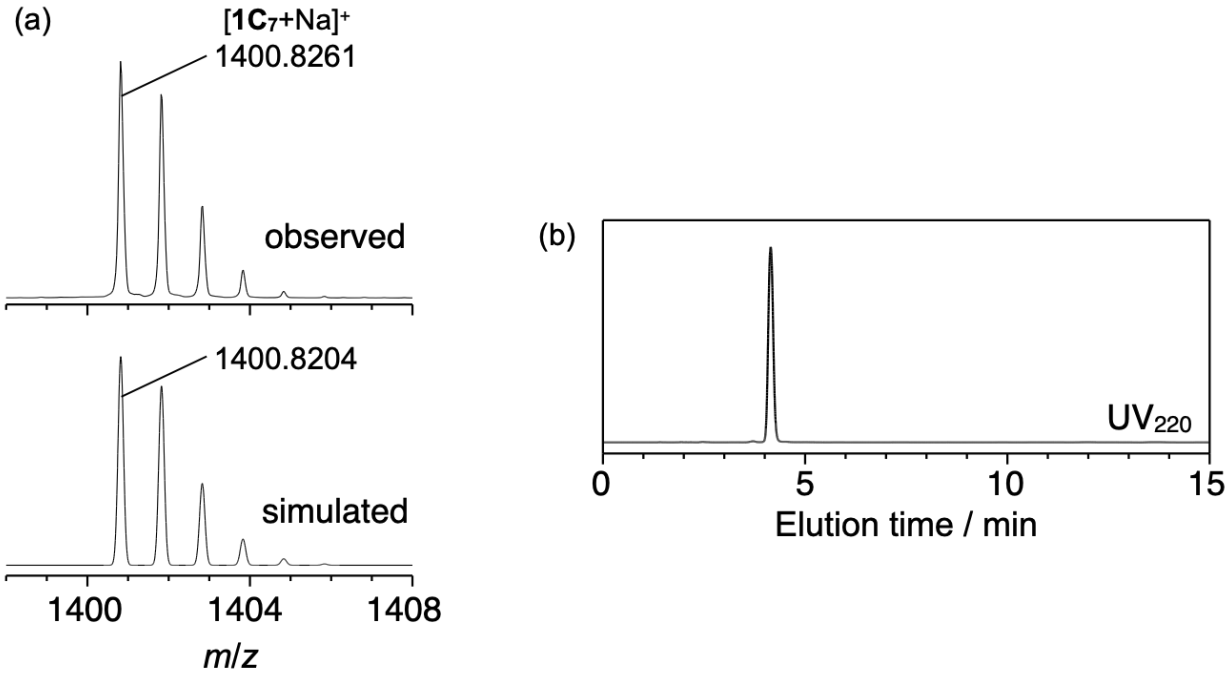

Figure S1. (a) Experimental (top) and simulated (bottom) electrospray ionization time-of-flight (ESI-TOF) mass spectrum of **1C**$_7$ and (b) UV (λ = 220 nm) detected HPLC chromatograms of **1C**$_7$. HPLC conditions: column, COSMOSIL 5C_{18}-MS-II (Nacalai Tesque, 0.46 (i.d.) × 25 cm); eluent, MeOH; flow rate, 2.0 mL/min; column temperature, room temperature.

4. Theoretical Studies on the Effects of Sequence and Chain Length of Non-Stapled Optically Inactive Peptides on the 3_{10}/α-Helix Propensity and on the Structures of the Stapled Peptide **1C$_7$**

Molecular modeling was performed on a Windows 11 PC with the ArgusLab software.[5] The initial structures of Ac-(Ac_6c)$_n$-$NHCH_3$ (n = 6–10 and 12), Ac-(Aib-Ac_6c)$_m$-Aib-$NHCH_3$ (m = 3–6), optically inactive nonapeptides composed of Aib and Ac_6c residues with different sequences, and **1C$_7$** were constructed according to the following procedures: the peptide backbones were set to be a standard (*P*)-α-helix ((ϕ, ψ, ω) = (–57º, –47º, 180º))[6-7] or a standard (*P*)-3_{10}-helix ((ϕ, ψ, ω) = (–60º, –30º, 180º))[8], except for the C-terminal Aib methyl ester residue of **1C$_7$** that took the opposite handedness ((ϕ, ψ, ω) = (+57º, +47º, 180º)) for (*P*)-α-helix, because the helix inversion at the C-terminus is often found in the analogous peptides.[9] In the initial structures of the 3_{10}- and/or α-helical oligopeptides, all the amide NH groups of the Ac_6c and Api residues were positioned in the axial orientation of the cyclohexyl and piperidine rings, respectively. However, for **1C$_7$**, the initial structures based on crystal structures (molecules A and B) placed the amide NH groups of some Ac_6c and Api residues in the equatorial position of the cyclohexyl and piperidine rings, respectively (see Figure 4). The alkyl crosslinker moieties (CO-C_5H_{10}-CO) in the initial structures of **1C$_7$** (except for those derived from crystal structures (molecules A and B)) were selectively geometry-optimized using molecular mechanics calculations (Universal force field (UFF) in ArgusLab software). The resulting structures were then fully optimized by the semi-empirical molecular orbital (MO) calculations (PM6 method[10] in MOPAC2016[11]) and the geometries were further refined by density functional theory (DFT) calculations using the dispersion corrected B3LYP (B3LYP-D3)[12] functional in *Gaussian* 16 software (Gaussian, Inc., Pittsburgh, PA).[13]

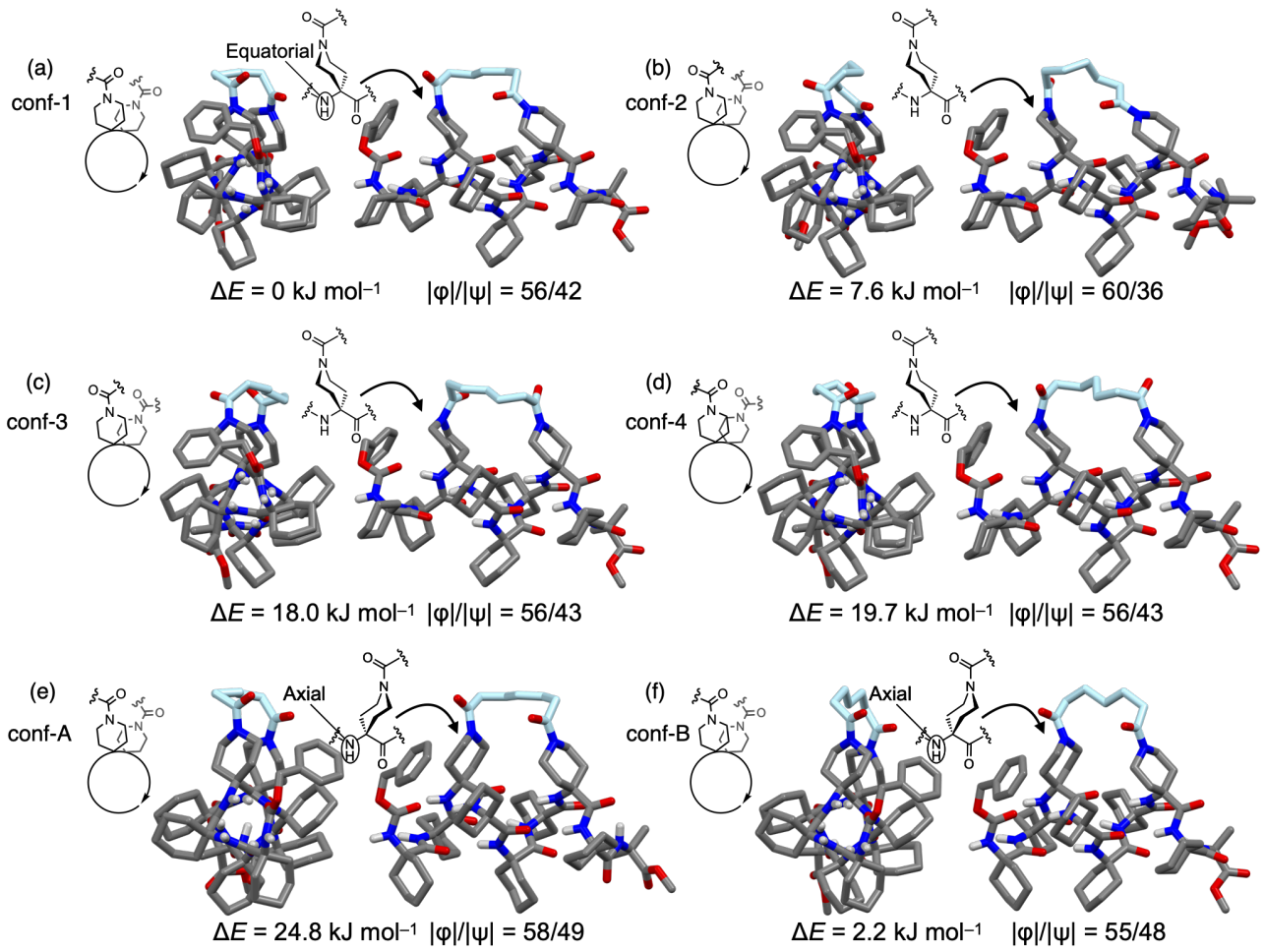

Figure S2. Top (left) and side (right) views of energy-minimized structures of (*P*)-α-helical **1C**$_7$ obtained by DFT calculations, based on different initial structures (**a**–**d**) conformations 1–4, derived from the standard (*P*)-α-helical conformation with four possible orientations of the side-chain amide carbonyl (–CO-N(CH$_2$)$_2$–) groups of the Api residues, and (**e**, **f**) conf-A and conf-B, derived from molecules A and B observed in the solid state. All of the hydrogen atoms except for the amide protons are omitted for clarity. Schematic representations of side-chain carbonyl orientations, energy difference (Δ*E*) values, and average dihedral angles (|ϕ|/|ψ|, in °, residues 1–8) are also shown. Detailed dihedral angles (ϕ, ψ and ω) and hydrogen-bonding parameters for these (*P*)-α-helical **1C**$_7$ structures are summarized in Tables S1–S12.

Table S1. Conformational angles (º) of (*P*)-α-helical **1C**$_7$ (conf-1) obtained by DFT calculation

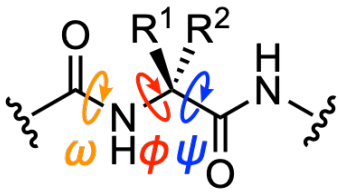

Residue (No.)	ϕ	ψ	ω
Ac_6c (1)	–60	–33	–168
Ac_6c (2)	–54	–34	–176
Api (3)	–50	–45	–176
Ac_6c (4)	–50	–51	–172
Ac_6c (5)	–56	–51	–175
Ac_6c (6)	–58	–44	–175
Api (7)	–61	–44	–174
Ac_6c (8)	–59	–36	–179
Aib (9)	50	42	175
|Average| (1)-(8)	174	56	42

Table S2. Parameters of the hydrogen bonds (Å, º) of (*P*)-α-helical **1C**$_7$ (conf-1) obtained by DFT calculation

Intramolecular H-bond Donor	Intramolecular H-bond Acceptor	N···O	H···O	N-H···O	C-O···H
N(1)	–				
N(2)	–				
N(3)	O(0)	3.016	2.030	163	128
N(4)	O(1)	3.083	2.154	151	122
N(5)	O(2)	3.172	2.372	135	112
N(6)	O(3)	3.087	2.467	119	103
N(7)	O(3)	3.050	2.090	157	161
N(8)	O(4)	3.235	2.294	154	151
N(9)	O(6)	3.202	2.417	134	97

Table S3. Conformational angles (º) of (*P*)-α-helical **1C**$_7$ (conf-2) obtained by DFT calculation

Residue (No.)	ϕ	ψ	ω
Ac_6c (1)	–61	–30	–169
Ac_6c (2)	–53	–33	–176
Api (3)	–50	–46	–175
Ac_6c (4)	–49	–52	–172
Ac_6c (5)	–57	–48	–174
Ac_6c (6)	–61	–39	–175
Api (7)	–65	–24	–174
Ac_6c (8)	–87	14	179
Aib (9)	52	35	–172
|Average| (1)-(8)	60	36	174

Table S4. Parameters of the hydrogen bonds (Å, º) of (*P*)-α-helical **1C**$_7$ (conf-2) obtained by DFT calculation

Intramolecular H-bond Donor	Intramolecular H-bond Acceptor	N···O	H···O	N-H···O	C-O···H
N(1)	–				
N(2)	–				
N(3)	O(0)	3.062	2.069	165	128
N(4)	O(1)	3.115	2.187	151	123
N(5)	O(2)	3.143	2.337	136	112
N(6)	O(3)	3.077	2.429	121	103
N(7)	O(3)	3.125	2.204	150	158
N(8)	O(5)	3.266	2.382	145	104
N(9)	O(6)	3.111	2.142	159	115

Table S5. Conformational angles (º) of (*P*)-α-helical **1C**$_7$ (conf-3) obtained by DFT calculation

Residue (No.)	ϕ	ψ	ω
Ac_6c (1)	–60	–29	–169
Ac_6c (2)	–50	–39	–179
Api (3)	–49	–49	–175
Ac_6c (4)	–55	–51	–171
Ac_6c (5)	–57	–50	–176
Ac_6c (6)	–57	–46	–175
Api (7)	–60	–44	–174
Ac_6c (8)	–61	–33	–178
Aib (9)	50	43	176
|Average| (1)-(8)	175	56	43

Table S6. Parameters of the hydrogen bonds (Å, º) of (*P*)-α-helical **1C**$_7$ (conf-3) obtained by DFT calculation

Intramolecular H-bond Donor	Intramolecular H-bond Acceptor	N···O	H···O	N-H···O	C-O···H
N(1)	–				
N(2)	–				
N(3)	O(0)	2.994	2.009	162	130
N(4)	O(1)	3.076	2.165	148	120
N(5)	O(2)	3.173	2.471	126	107
N(6)	O(2)	3.225	2.240	163	160
N(7)	O(3)	3.121	2.160	157	155
N(8)	O(4)	3.320	2.401	150	149
N(9)	O(6)	3.154	2.323	139	100

Table S7. Conformational angles (º) of (*P*)-α-helical **1C**$_7$ (conf-4) obtained by DFT calculation

Residue (No.)	ϕ	ψ	ω
Ac_6c (1)	–61	–29	–168
Ac_6c (2)	–49	–41	–179
Api (3)	–50	–51	–174
Ac_6c (4)	–55	–50	–171
Ac_6c (5)	–55	–49	–175
Ac_6c (6)	–57	–47	–175
Api (7)	–65	–43	–174
Ac_6c (8)	–59	–36	–179
Aib (9)	50	42	178
|Average| (1)-(8)	174	56	43

Table S8. Parameters of the hydrogen bonds (Å, º) of (*P*)-α-helical **1C**$_7$ (conf-4) obtained by DFT calculation

Intramolecular H-bond Donor	Intramolecular H-bond Acceptor	N···O	H···O	N-H···O	C-O···H
N(1)	–				
N(2)	–				
N(3)	O(0)	3.000	2.021	161	129
N(4)	O(1)	3.097	2.229	143	117
N(5)	O(2)	3.207	2.549	122	103
N(6)	O(2)	3.291	2.316	161	158
N(7)	O(3)	3.232	2.283	155	154
N(8)	O(4)	3.105	2.150	156	156
N(9)	O(5)	3.247	2.398	141	144

Table S9. Conformational angles (º) of (*P*)-α-helical **1C$_7$** (conf-A) obtained by DFT calculation

Residue (No.)	ϕ	ψ	ω
Ac$_6$c (1)	–53	–48	–163
Ac$_6$c (2)	–54	–50	–174
Api (3)	–55	–54	–176
Ac$_6$c (4)	–53	–49	–176
Ac$_6$c (5)	–55	–54	–174
Ac$_6$c (6)	–58	–42	–172
Api (7)	–58	–45	–179
Ac$_6$c (8)	–77	49	179
Aib (9)	–53	–39	–175
|Average| (1)-(8)	58	49	174

Table S10. Parameters of the hydrogen bonds (Å, º) of (*P*)-α-helical **1C$_7$** (conf-A) obtained by DFT calculation

Intramolecular H-bond Donor	Intramolecular H-bond Acceptor	N···O	H···O	N-H···O	C-O···H
N(1)	–				
N(2)	–				
N(3)	O(0)	2.916	2.083	138	121
N(4)	O(0)	3.274	2.291	163	156
N(5)	O(1)	3.100	2.111	164	158
N(6)	O(2)	3.201	2.235	159	153
N(7)	O(3)	3.278	2.375	148	152
N(8)	O(4)	3.294	2.404	146	150
N(9)	O(7)	2.933	1.998	152	90

Table S11. Conformational angles (º) of (*P*)-α-helical **1C$_7$** (conf-B) obtained by DFT calculation

Residue (No.)	ϕ	ψ	ω
Ac$_6$c (1)	–52	–50	–164
Ac$_6$c (2)	–51	–52	–173
Api (3)	–51	–56	–177
Ac$_6$c (4)	–54	–50	–174
Ac$_6$c (5)	–55	–49	–175
Ac$_6$c (6)	–56	–46	–175
Api (7)	–61	–45	–175
Ac$_6$c (8)	–60	–35	–178
Aib (9)	50	42	176
|Average| (1)-(8)	55	48	174

Table S12. Parameters of the hydrogen bonds (Å, º) of (*P*)-α-helical **1C$_7$** (conf-B) obtained by DFT calculation

Intramolecular H-bond Donor	Intramolecular H-bond Acceptor	N···O	H···O	N-H···O	C-O···H
N(1)	–				
N(2)	–				
N(3)	O(0)	2.931	2.112	136	122
N(4)	O(0)	3.337	2.360	162	154
N(5)	O(1)	3.110	2.118	165	163
N(6)	O(2)	3.135	2.163	160	156
N(7)	O(3)	3.239	2.303	153	154
N(8)	O(4)	3.236	2.292	154	155
N(9)	O(5)	3.271	2.441	139	146

5. X-ray Crystallographic Analysis of $\mathbf{1C_7}$

Crystals of $\mathbf{1C_7}$ suitable for single-crystal X-ray diffraction were obtained by slow evaporation of a CH_3CN/CH_2Cl_2 solution of $\mathbf{1C_7}$ at room temperature. A colorless single crystal with dimensions 0.18 × 0.15 × 0.07 mm^3 was selected for intensity measurements. The X-ray diffraction data for $\mathbf{1C_7}$ were collected on a Bruker Venture D8 diffractometer with Cu-Kα radiation (λ = 1.54178 Å) at 100 K. The data were corrected for Lorentz and polarization factors and for absorption by semiempirical methods based on symmetry-equivalent and repeated reflections. The structure was solved by direct methods (SHELXD[14]) and refined by full-matrix least squares on F^2 using SHELXL 2014[15]. All non-hydrogen atoms were refined anisotropically. All hydrogen atoms were calculated geometrically and refined using the riding models. The X-ray crystallographic data for the structure of $\mathbf{1C_7}$ has been deposited at the Cambridge Crystallographic Data Centre (CCDC) under deposition number 2421064.

Table S13. Conformational angles (º) of (*P*)-α-helical **1C**$_7$ (molecule A)

Residue (No.)	ϕ	ψ	ω
Ac_6c (1)	–56	–50	–172
Ac_6c (2)	–48	–56	–175
Api (3)	–55	–54	–170
Ac_6c (4)	–55	–48	–175
Ac_6c (5)	–51	–53	–175
Ac_6c (6)	–58	–39	–172
Api (7)	–60	–35	–174
Ac_6c (8)	–76	–16	–173
Aib (9)	–56	–46	–161
|Average| (1)-(8)	57	44	173

Table S14. Parameters of the hydrogen bonds (Å, º) of (*P*)-α-helical **1C**$_7$ (molecule A)

Intramolecular H-bond Donor	Intramolecular H-bond Acceptor	N···O	H···O	N-H···O	C-O···H
N(1)	–				
N(2)	–				
N(3)	O(0)	2.977	2.49	116	113
N(4)	O(0)	3.163	2.29	171	162
N(5)	O(1)	3.032	2.16	170	167
N(6)	O(2)	3.299	2.45	163	157
N(7)	O(4)	3.108	2.52	125	106
N(8)	O(5)	3.103	2.39	138	111
N(9)	O(6)	3.243	2.39	164	113

Table S15. Conformational angles (º) of (*P*)-α-helical **1C**$_7$ (molecule B)

Residue (No.)	ϕ	ψ	ω
Ac_6c (1)	–52	–53	–169
Ac_6c (2)	–47	–56	–176
Api (3)	–49	–57	–176
Ac_6c (4)	–54	–52	–174
Ac_6c (5)	–56	–48	–172
Ac_6c (6)	–59	–44	–172
Api (7)	–57	–38	–172
Ac_6c (8)	–75	–23	–172
Aib (9)	48	36	–163
|Average| (1)-(8)	56	46	173

Table S16. Parameters of the hydrogen bonds (Å, º) of (*P*)-α-helical **1C**$_7$ (molecule B)

Intramolecular H-bond Donor	Intramolecular H-bond Acceptor	N···O	H···O	N-H···O	C-O···H
N(1)	–				
N(2)	–				
N(3)	O(0)	3.021	2.57	113	114
N(4)	O(0)	3.269	2.40	168	159
N(5)	O(1)	3.030	2.16	173	171
N(6)	O(2)	3.133	2.28	164	161
N(7)	O(3)	3.302	2.48	157	155
N(8)	O(5)	3.225	2.52	137	109
N(9)	O(6)	3.205	2.36	162	110

6. Kinetic and Thermodynamic Analyses of the *P*/*M* Interconversion of $\mathbf{1C_7}$

The free energy of activation ($\Delta G^{\ddagger}$, J mol^{-1}) for the interconversion between the (*P*) and (*M*)-α-helical $\mathbf{1C_7}$ and the rate constant for the *P*/*M* interconversion (k, sec^{-1}) are given by the following equations.

$$\Delta G^{\ddagger} = RT_c\ln[2^{1/2}k_BT_c/\pi h(\Delta\nu)] \quad (1)$$

$$k = (k_BT/h)\exp(-\Delta G^{\ddagger}/RT) \quad (2)$$

where T_c is the coalescence temperature and $\Delta\nu$ (Hz) is the frequency difference between the N-terminal methylene signals in the ^{1}H NMR spectrum.

From Figure 3,

$\Delta\nu = (5.242–5.070) \times 600$ MHz = 103.2 Hz

$T_c = 373$ K

By using equations (1) and (2),

$\Delta G^{\ddagger} = RT_c\ln[2^{1/2}k_BT_c/\pi h(\Delta\nu)] = 75.2$ kJ/mol

$k_{298} = (k_BT/h)\exp(-\Delta G^{\ddagger}/RT) = 0.41$ sec^{-1}

7. ^{1}H and ^{13}C NMR Spectra

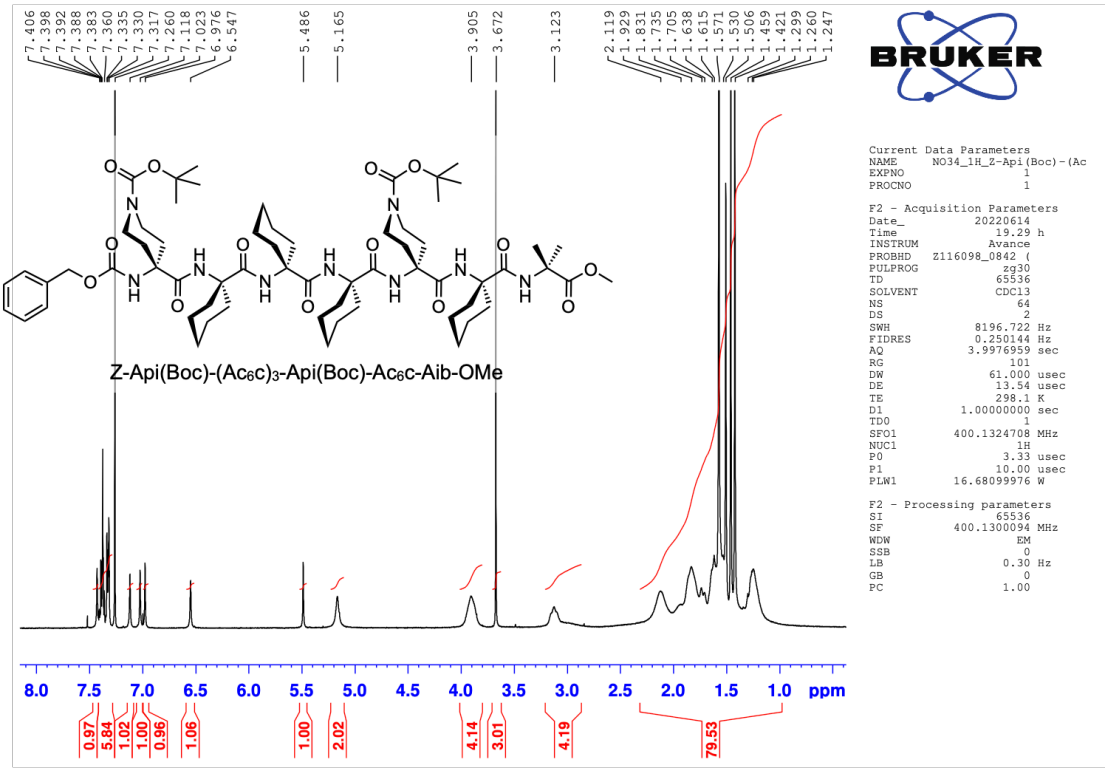

Figure S3. ^{1}H NMR spectrum (400 MHz, $CDCl_3$, 25 ºC) of Z-Api(Boc)-(Ac$_6$c)$_3$-Api(Boc)-Aib-OMe.

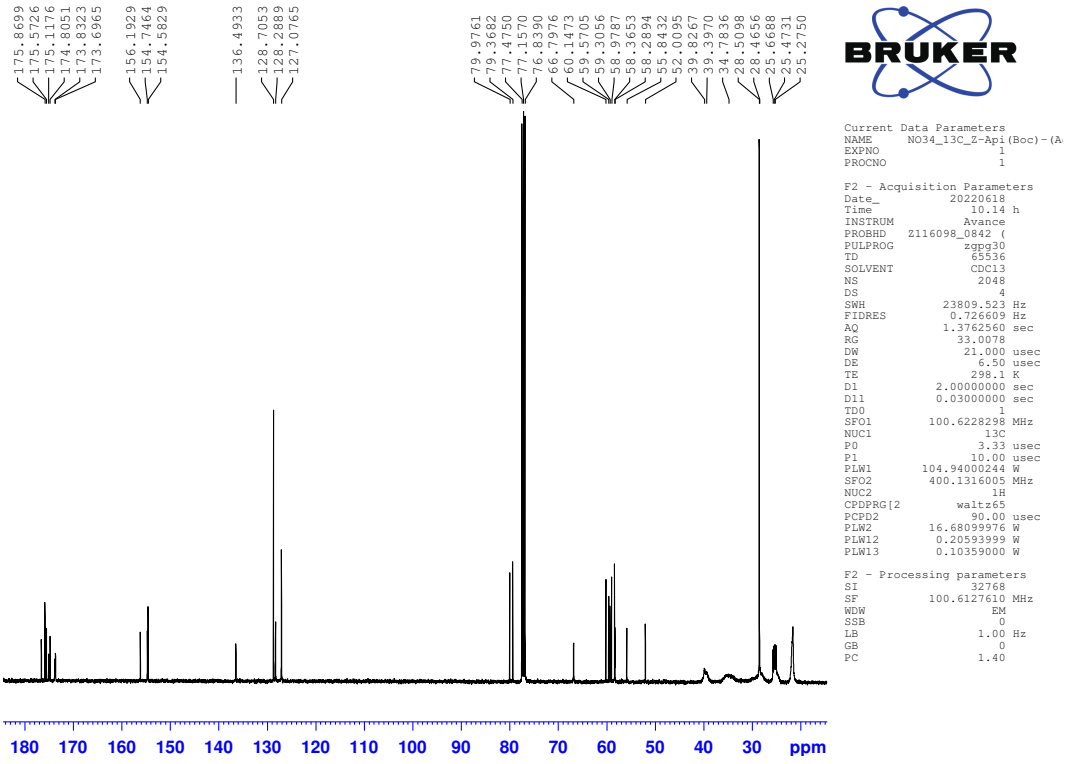

Figure S4. ^{13}C NMR spectrum (100 MHz, $CDCl_3$, 25 ºC) of Z-Api(Boc)-(Ac$_6$c)$_3$-Api(Boc)-Aib-OMe.

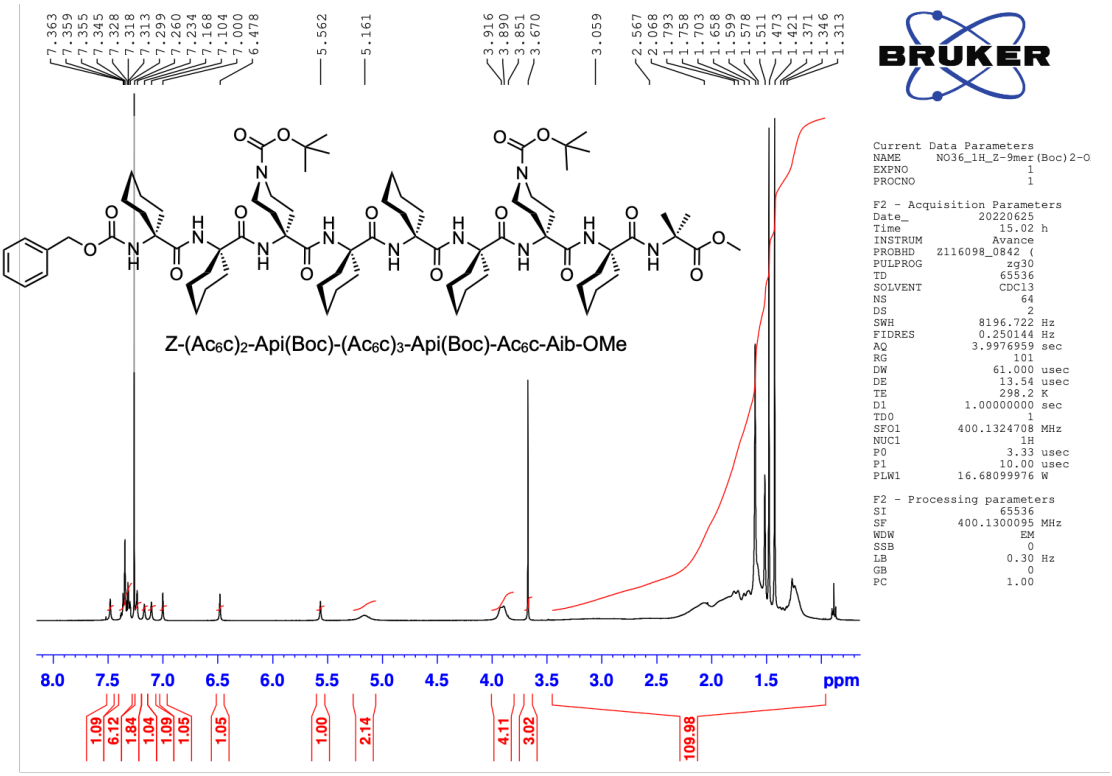

Figure S5. ^{1}H NMR spectrum (400 MHz, $CDCl_3$, 25 ºC) of Z-(Ac$_6$c)$_2$-Api(Boc)-(Ac$_6$c)$_3$-Api(Boc)-Aib-OMe.

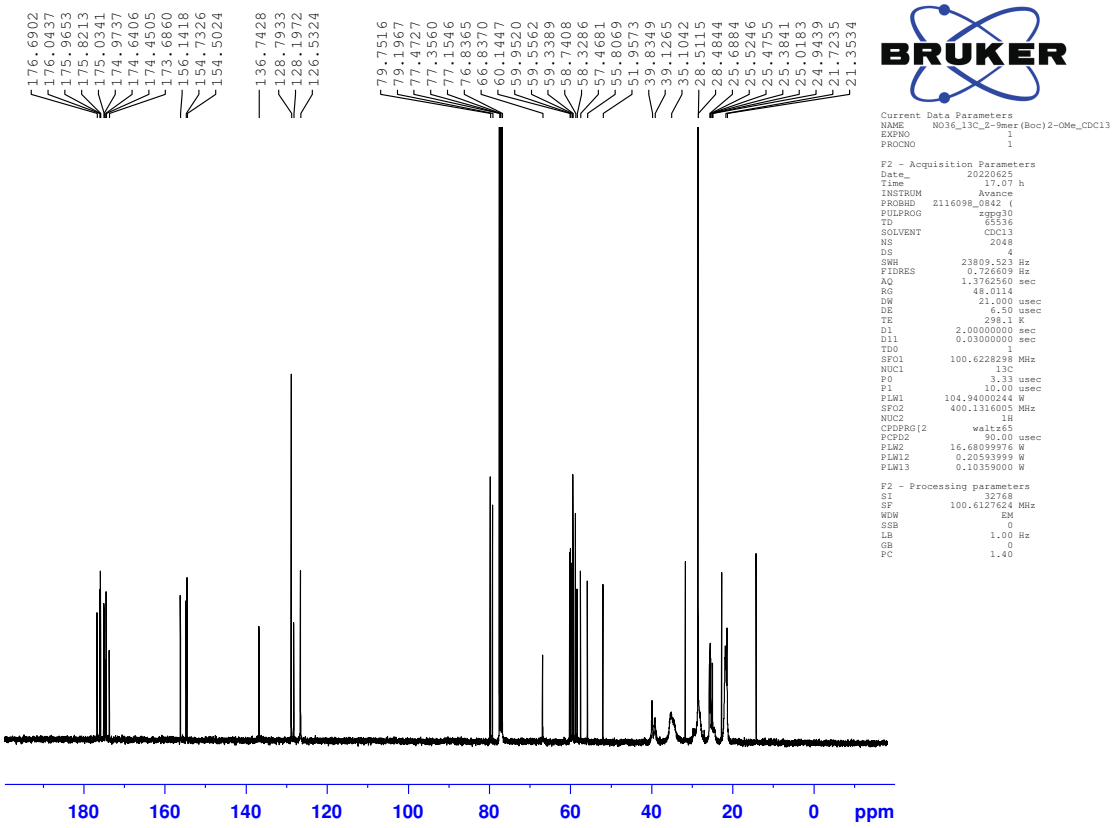

Figure S6. ^{13}C NMR spectrum (100 MHz, $CDCl_3$, 25 ºC) of Z-(Ac$_6$c)$_2$-Api(Boc)-(Ac$_6$c)$_3$-Api(Boc)-Aib-OMe.

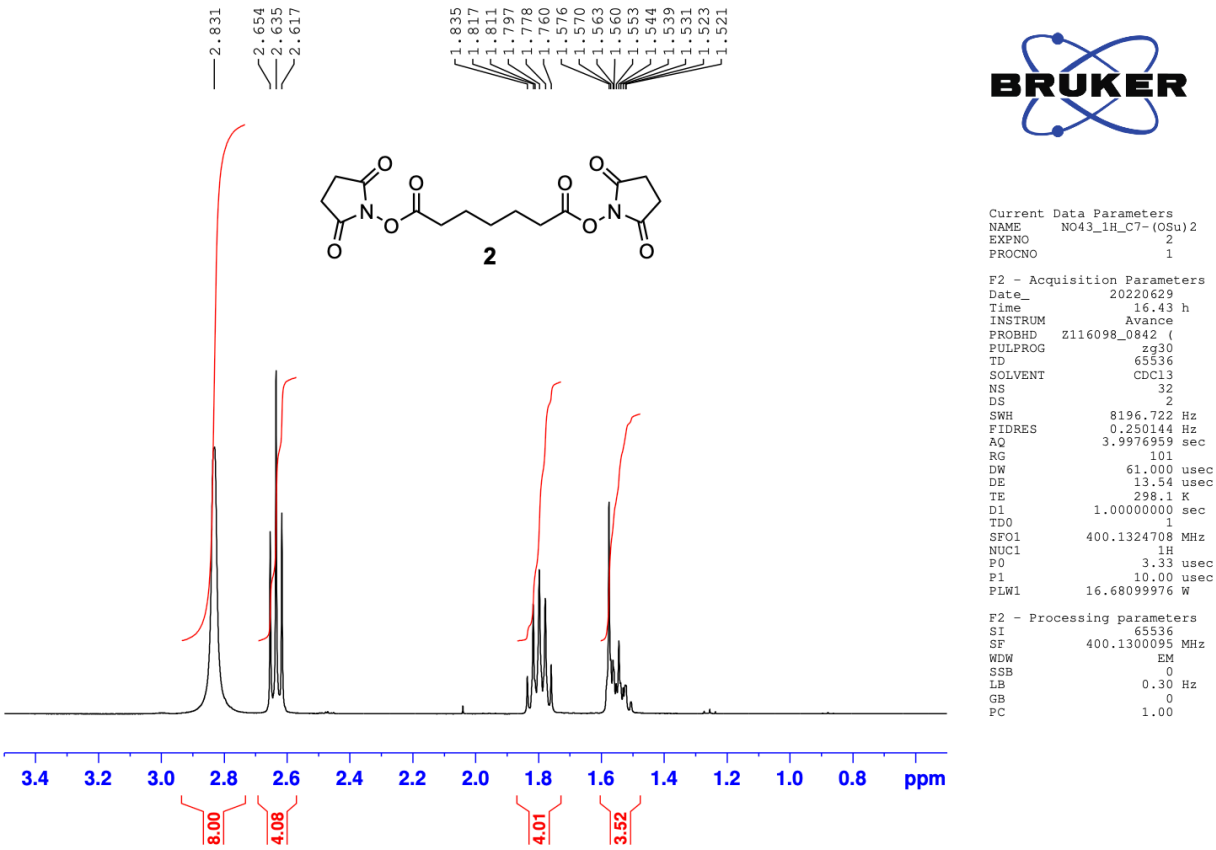

Figure S7. ^{1}H NMR spectrum (400 MHz, $CDCl_3$, 25 ºC) of **2**. The peak at 1.4-1.6 ppm overlaps with water in $CDCl_3$.

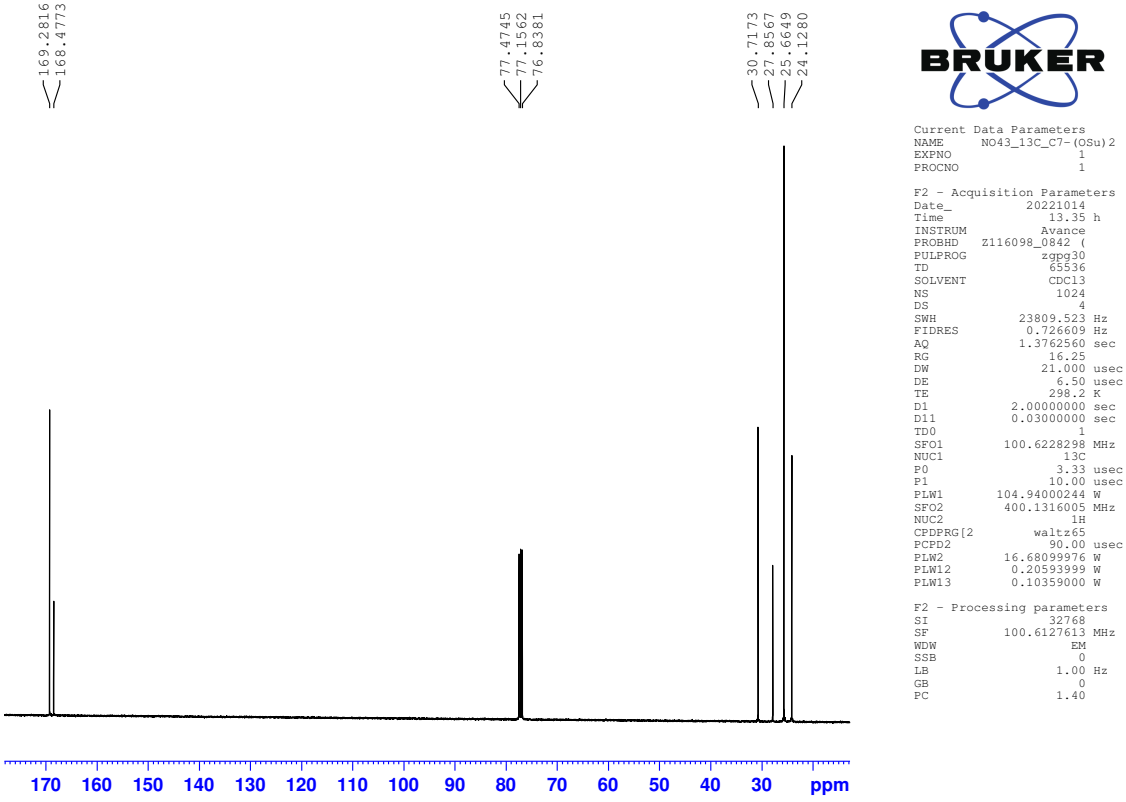

Figure S8. ^{13}C NMR spectrum (100 MHz, $CDCl_3$, 25 ºC) of **2**.

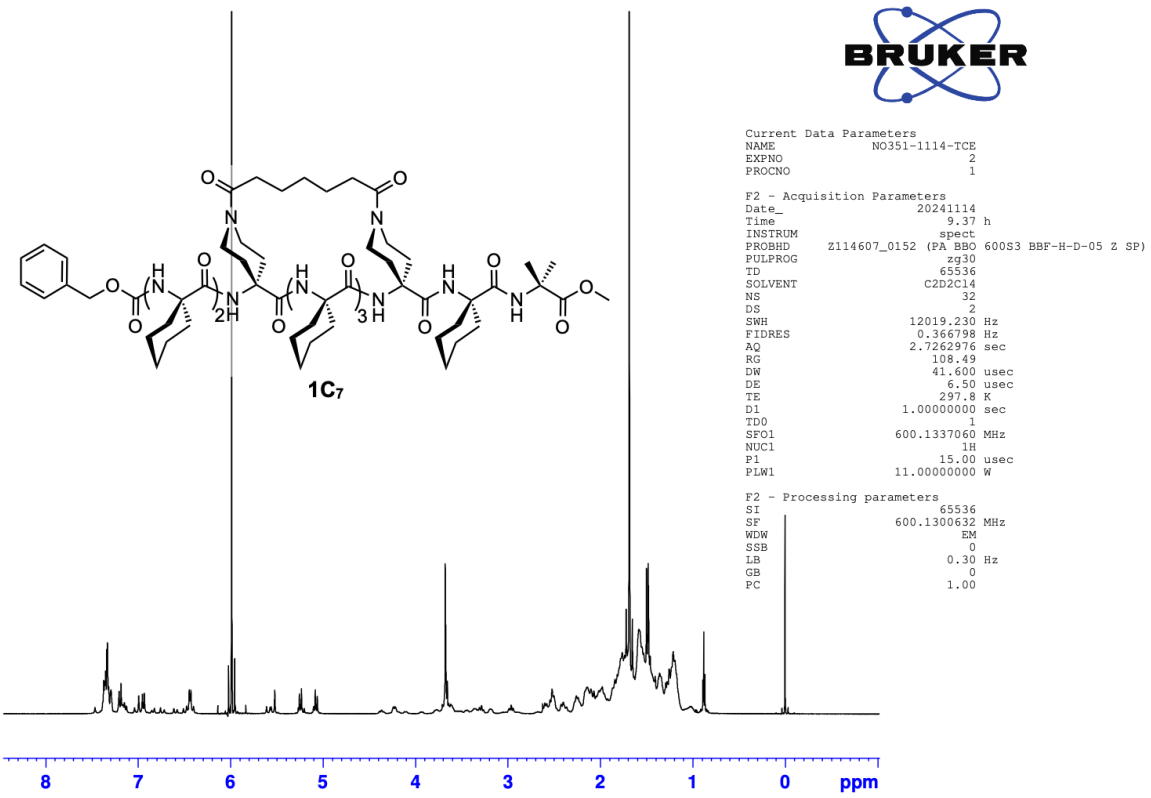

Figure S9. ^{1}H NMR spectrum (600 MHz, $C_2D_2Cl_4$, 25 ºC) of **1C$_7$**.

8. Supporting References

1. M. Crisma, G. M. Bonora, C. Toniolo, A. Bavoso, E. Benedetti, B. Di Blasio, V. Pavone and C. Pedone, *Macromolecules*, 1988, **21**, 2071.

2. N. Ousaka, M. J. MacLachlan and S. Akine, *Nat. Commun.*, 2023, **14**, 6834.

3. A. El-Faham, R. S. Funosas, R. Prohens and F. Albericio, *Chem. - Eur. J.*, 2009, **15**, 9404.

4. A. El-Faham and F. Albericio, *J. Pep. Sci.*, 2010, **16**, 6.

5. M. Thompson, *ArgusLab, Planaria Software LLC, Seattle, WA*, 1996.

6. S. Arnott and A. J. Wonacott, *J. Mol. Biol.*, 1966, **21**, 371.

7. S. Arnott and S. D. Dover, *J. Mol. Biol.*, 1967, **30**, 209.

8. C. Toniolo and E. Benedetti, *Trends Biochem. Sci.*, 1991, **16**, 350.

9. E. Benedetti, M. Saviano, R. Iacovino, C. Pedone, A. Santini, M. Crisma, F. Formaggio, C. Toniolo, Q. B. Broxterman and J. Kamphuis, *Biopolymers*, 1998, **46**, 433.

10. J. J. P. Stewart, *J. Mol. Model.*, 2007, **13**, 1173.

11. J. J. P. Stewart, *MOPAC2012, Stewart Computational Chemistry, Colorado Springs, CO, USA,* http://openmopac.net/, 2012.

12. S. Grimme, J. Antony, S. Ehrlich and H. Krieg, *J. Chem. Phys.*, 2010, **132**, 154104.

13. Gaussian 16, Revision C.01, M. J. Frisch, G. W. Trucks, H. B. Schlegel, G. E. Scuseria, M. A. Robb, J. R. Cheeseman, G. Scalmani, V. Barone, G. A. Petersson, H. Nakatsuji, X. Li, M. Caricato, A. V. Marenich, J. Bloino, B. G. Janesko, R. Gomperts, B. Mennucci, H. P. Hratchian, J. V. Ortiz, A. F. Izmaylov, J. L. Sonnenberg, Williams, F. Ding, F. Lipparini, F. Egidi, J. Goings, B. Peng, A. Petrone, T. Henderson, D. Ranasinghe, V. G. Zakrzewski, J. Gao, N. Rega, G. Zheng, W. Liang, M. Hada, M. Ehara, K. Toyota, R. Fukuda, J. Hasegawa, M. Ishida, T. Nakajima, Y. Honda, O. Kitao, H. Nakai, T. Vreven, K. Throssell, J. A. Montgomery Jr., J. E. Peralta, F. Ogliaro, M. J. Bearpark, J. J. Heyd, E. N. Brothers, K. N. Kudin, V. N. Staroverov, T. A. Keith, R. Kobayashi, J. Normand, K. Raghavachari, A. P. Rendell, J. C. Burant, S. S. Iyengar, J. Tomasi, M. Cossi, J. M. Millam, M. Klene, C. Adamo, R. Cammi, J. W. Ochterski, R. L. Martin, K. Morokuma, O. Farkas, J. B. Foresman and D. J. Fox, Gaussian, Inc., Wallingford, CT, 2016.

14. G. M. Sheldrick, *SHELXD-2002, Program for crystal structure determination, University of Göttingen*, 2002.

15. G. M. Sheldrick, *Acta Cryst.*, 2015, **C71**, 3.